JOURNAL OF AIRCRAFT
Vol. 39, No. 2, March–April 2002

Turbulent Near-Wake Studies Behind an Infinitely Swept Wing

N. Subaschandar*
National Aerospace Laboratories, Bangalore 560 017, India
and
A. Prabhu†
Indian Institute of Science, Bangalore 560 012, India

The three-dimensional asymmetric turbulent near-wake behind an infinitely swept wing with GAW(2) airfoil has been investigated at low speeds. The near-wake in the present study is asymmetric because the boundary layers on the top and bottom surfaces of the model develop under different streamwise pressure gradients. Distributions of mean velocity, three turbulent normal stresses, and two important Reynolds shear stresses have been measured using hot-wire anemometry. The profiles of mean velocity and Reynolds shear stress exhibit asymmetry near the trailing edge and seem to have become symmetric within a short distance of 60 trailing edge momentum thicknesses. Results of computation using K–ε turbulence model with a simple scheme to predict the near-wake behind the swept wing have also been presented and compared with the experimental data. The agreement of the predicted mean flow development with the experiment is fair considering the simplicity of the scheme.

Nomenclature

b = sum of the wake half-thicknesses based on u, in the upper and lower layers of the wake
C_f = skin friction coefficient
C_p = pressure coefficient
c = chord length of the model
H = shape factor based on u
K = turbulent kinetic energy
U_e = mean velocity at the edge of the wake along x axis
U_∞ = undisturbed tunnel freestream velocity
u = component of mean velocity along x axis
u_m = minimum value of u in the wake
$\langle u'v' \rangle$, $\langle u'w' \rangle$ = Reynolds shear stress components
$\langle u'^2 \rangle$, $\langle v'^2 \rangle$, $\langle w'^2 \rangle$ = turbulent normal stress components
v = component of mean velocity along y axis
w = component of mean velocity along z axis
x = tunnel freestream direction
y = normal to the model and perpendicular to x axis
z = spanwise direction
δ^* = sum of the displacement thicknesses based on u, in the upper and lower layers of the wake
ε = dissipation rate of turbulent kinetic energy
θ = sum of the momentum thicknesses based on u, in the upper and lower layers of the wake
θ_T = sum of the momentum thicknesses on the top and bottom surfaces close to the trailing edge
ν_τ = eddy viscosity

Received 22 December 2000; revision received 30 October 2001; accepted for publication 17 November 2001.

*Scientist, Experimental Aerodynamics Division; currently Mechanical Engineer, Advanced Mechanical Engineering, GE India Technology Center, Bangalore, 560-066, India.

†Professor, Department of Aerospace Engineering.

Introduction

NUMEROUS studies have addressed the problem of turbulent near-wake development behind two-dimensional flat plates and airfoils at low speeds.[1–3] It is in the near-wake region that the boundary layers, separated by the body surface, merge to develop into a single free shear layer, which does not have any rigid boundary conditions. To estimate the drag on the body, it becomes necessary to evaluate the wake parameters at the downstream edge of this region. The evaluation of the flow in this region thus represents an important aerodynamic problem related to lift and drag.

The present study is concerned with the development of three-dimensional turbulent near-wake behind an infinitely swept wing. Most earlier studies have dealt with symmetric three-dimensional turbulent near-wake flows behind a swept flat plate[4] or a swept wing.[5] Subaschandar and Prabhu[4] carried out extensive studies in the near-wake behind an infinitely swept flat plate at zero incidence. Their studies have shown that the law of the wall, which was found to be valid in the three-dimensional turbulent boundary layers, continues to be valid for some more distance in the near-wake, and the wall layer coordinates can be used to describe the mean velocity profiles in the near-wake. They further extended their work on the two-layer theory for a two-dimensional near-wake[4,6] using the method of matched asymptotic expansions to the turbulent near-wake flow behind an infinitely swept flat plate.[7] Novak and Ramaprian[5] carried out measurements in the symmetric wake of an infinitely swept wing with 30-deg sweep and at zero incidence. In the context of three-dimensional asymmetric turbulent near-wake flows, Cousteix and Pailhas[8] presented measurements behind a symmetric airfoil with an ONERA D cross section with a sweep angle of 22.5 deg and at an incidence of 8 deg where the boundary layer on the suction side of the airfoil was nearly separated because of the strong streamwise adverse pressure gradients. They measured mean velocity and all six components of Reynolds shear stress tensor using a slanted wire, x-wire and four-wire probes. The experiments were made in a relatively small tunnel, which provided a model aspect ratio of only 2.0 and the blockage was close to 10%. As a result the investigators made near-wake measurements at five spanwise stations also. The data on the vertical median of the wind tunnel were reported.[8] The mean velocity profiles showed a tendency toward symmetry at about a distance of 70 trailing edge momentum thicknesses, and an analysis of the results revealed that the vector of components ($\langle u'v' \rangle$, $\langle v'w' \rangle$) was nearly aligned with the y derivative of mean velocity.[8] It is clear that the flow investigated by Cousteix and Pailhas[8] is quite complex with strong three-dimensionality and should be a challenge for turbulence models and numerical prediction techniques.

In the present paper a three-dimensional asymmetric turbulent near-wake flow, which is considerably less complex compared to the flow investigated by Cousteix and Pailhas,[8] is documented. The experiments were performed in the asymmetric turbulent near-wake behind an infinitely swept wing with a GAW(2) airfoil cross section at zero incidence. The airfoil is cambered with the boundary layers on the top and bottom surfaces develop under different streamwise pressure gradients and are attached at the trailing edge. Three mean velocity components, three turbulent normal stress components, and two Reynolds shear stress components have been measured in the swept asymmetric near-wake. An engineering prediction of the near-wake flow, using $K-\varepsilon$ turbulence model, has been carried out. In this paper results of experimental work and an engineering prediction scheme are presented. The near-wake flow studied here, being significantly three-dimensional and yet relatively simple, is expected to provide a broad understanding of asymmetric near-wake flow features and present a good and critical test of the capabilities of turbulence models, which take into account the three-dimensionality of the flow.

Experimental Setup and Procedure

Wind Tunnel and Model Configuration

Experiments were carried out in the 1.5×1.5-m open circuit wind tunnel. The tunnel has a contraction ratio of 12:1. The tunnel velocity can be varied in the range 5–50 m/s, and the freestream turbulence level at the maximum speed is within 0.12%. Figure 1 gives schematic of the model configuration and the coordinate system used. The wing model has a 13.6% thick GAW(2) profile with a chord of 450 mm and a sweep angle of 25 deg and was held horizontally between the test section walls. The basic GAW(2) profile has a blunt trailing edge with a trailing edge thickness to chord ratio of 0.005. To avoid possible flow complexities associated with a blunt base, the trailing edge was made sharp by extending it by 30 mm. The model was instrumented with 48 static pressure taps of outer diameter 1.2 mm each on both upper and the lower surfaces along the midspan in the direction of the freestream. The boundary layers on the upper and lower surfaces of the model were tripped at 10% chord from the leading edge using transition trips (sandpaper of width 15 mm and grade 50).

Measurements

All of the measurements were made at a freestream velocity of 30 m/s providing a chord Reynolds number of 0.75×10^6. Surface pressure measurements were made using a low-pressure range Setra Transducer (0–0.2 psi range) and Furnace Control Micromanometers. Two 48-port Scannivalves were utilized for measuring pressure distributions on the model. All of the data were acquired and processed using a PC 486 system. Hot-wire anemometry has been widely used for mean velocity and turbulence measurements. An X-wire hot-wire probe has been used in the present measurements because the tunnel freestream direction is the predominant mean flow direction. Hot-wire measurements were made using DISA 55M01 Constant Temperature Anemometers with Tungsten wire sensors (1 mm active wire length). The diameter of the sensors was 5 μm, and sensor spacing was about 1 mm. Measurements were made by keeping the probe in two orientations. The mean velocity components u and v, two turbulent normal stress components $\langle u'^2 \rangle$ and $\langle v'^2 \rangle$, and the Reynolds shear stress component $\langle u'v' \rangle$ were measured by keeping the wires in the vertical plane. The mean velocity component w, turbulent normal stress component $\langle w'^2 \rangle$, and the other Reynolds shear stress component $\langle u'w' \rangle$ were measured by keeping the wires in the horizontal plane. It was found in an earlier study[9] that the surface streamline deviation on the upper and lower surfaces of the model is less than 10 deg even at the trailing edge. Hence measurements were taken along the tunnel freestream direction and not along the streamlines.

Initial Conditions

The development of wake behind any streamlined body depends on the initial conditions of the flow at the trailing edge. The values of displacement thickness, momentum thickness, shape factor, and skin friction coefficient, for both upper and lower surfaces, at the trailing edge are given in Table 1.

The profiles of streamwise component of mean velocity were measured at three different spanwise stations close to the trailing edge in the near-wake (at $x = 1.5$ mm). The measurements showed very little difference among the profiles as can be seen from the Fig. 2, confirming the existence of infinite sweep condition in the flow.

Accuracy of the Measured Data

The uncertainties in x-wire measurements arise from a variety of sources including finite probe size, error in the measurement of angle between the wires, out-of-plane velocity components, temperature drift, and calibration inaccuracies. The last two uncertainty sources were minimized by repeated calibration. Uncertainties in the measured data are estimated by using the method of Kline and McClintock[10] and taking repeatability into account. The uncertainty estimates in the measurements of C_p, u, $\langle u'^2 \rangle$, and $\langle u'v' \rangle$ were supported by comparing data with the profiles of Sundaram et al.[9] They carried out measurements of C_p distribution on the model and $\langle u'^2 \rangle$ and $\langle u'v' \rangle$ in the upstream boundary layer close to the trailing edge under similar experimental conditions. The hot-wire sensors were

Table 1 Parameters at the trailing edge

Parameter >	δ^*, mm	θ, mm	H	C_f
Upper surface	3.6	2.1	1.534	0.0026
Lower surface	0.8	0.5	1.416	0.0042

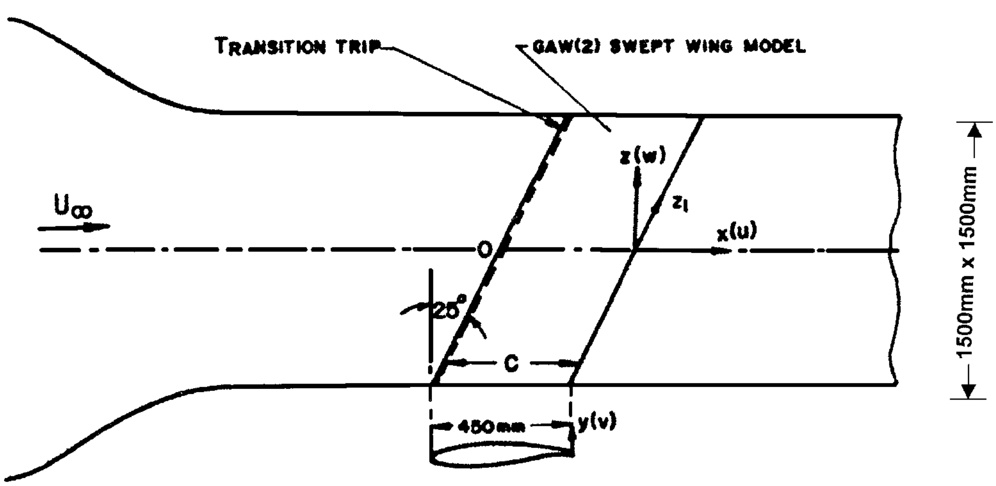

Fig. 1 Schematic of the experimental setup, model, and coordinate system.

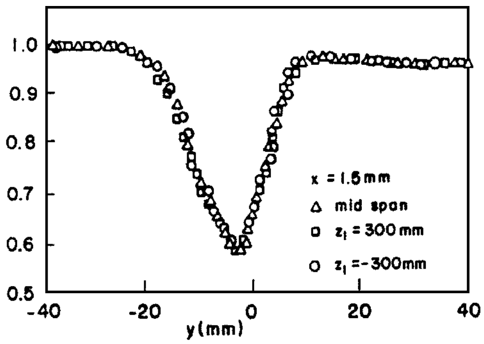

Fig. 2 Distribution of mean velocity profiles at three stations along the trailing edge (check for infinite sweep condition).

calibrated both before and after measurement of each wake profile. The error in the estimation of the calibration constants for the sensors with repeated runs was within ±2%. The uncertainties in the pressure coefficient C_p and mean velocity components u, v, w are estimated to be within ±0.5 and ±2% of corresponding local values. The uncertainty in the normal stresses was estimated to be less than ±4% of the local values of the corresponding normal stresses. This estimate was supported by comparison of $\langle u'^2\rangle$ data measured in the upstream boundary layer with that of Sundaram et al.[9] Agreement of $\langle u'^2\rangle$ profiles was good beyond $y/\delta = 0.15$. Below this location finite-probe-size effects become important. The active length of each wire was about 40–50 viscous wall units. This length would be expected to cause some attenuation of the normal stresses near the wall. The estimated uncertainty in the measurement of shear stress components $\langle u'v'\rangle$ and $\langle u'w'\rangle$ was ±8% of the local values. The uncertainty apparently increased rapidly on approaching the wall. This estimate in the uncertainty of shear stress components was supported by comparison of $\langle u'v'\rangle$ profile with data of Sundaram et al.[9] $\langle u'v'\rangle$ profiles agreed within a few percentage across the boundary layer except in a region close to the wall. Because the estimates are given in the boundary layer close to the trailing edge, it is believed that the uncertainties, in the wake flow will not be more than the estimates given here.

Engineering Prediction of Flow

Computation of a three-dimensional turbulent near-wake flow is complex because of the presence of the spanwise component of mean velocity and the need to model at least two Reynolds shear stress components. For the present flow there is need to model the asymmetric nature of the flow as well. A simple engineering calculation method has been used to predict the three-dimensional turbulent near-wake behind a swept wing. The following assumptions were made in carrying out the computations:

1) Computations were carried out by splitting the wake into two layers: one layer above and the other layer below the minimum velocity line in the wake.

2) The two layers were computed separately.

3) Computations were carried out in the direction normal to the trailing edge because of the simplicity of equations.

4) Standard K–ε turbulence model has been used to model Reynolds shear stress terms.

5) Boundary layer equations were used.

6) Pressure variations in the normal and streamwise directions were neglected.

7) Computations were started at the streamwise station $x = 1.5$ mm ($x/\theta_T = 0.6$).

8) Normal derivatives of velocity components were taken to be zero at the minimum velocity line.

Complete details of the engineering prediction scheme are given in Subaschandar and Prabhu.[11] Because the computations were carried out in the direction normal to the trailing edge, the values of mean velocity and Reynolds shear stress along the freestream direction are calculated using the sweep angle, before making comparison with the experimental results.

Results and Discussion

Figure 3 shows the static pressure distribution on both the suction and pressure sides of the model along its chord length. C_p distribution on the model indicates that the boundary layer is only under a moderate adverse streamwise pressure gradient and the flow is attached near the trailing edge. These observations are supported by the fact, as it will be seen later, that the shape parameter has a value of about 1.5 at the trailing edge. Figure 4 shows the development of the streamwise component of the mean velocity profiles at various streamwise locations in the wake. The profiles are asymmetric with respect to the x axis and also the location of the minimum velocity starts shifting toward the lower side of the wake as the streamwise distance increases. Mean velocity profiles show a tendency toward symmetrization of the velocity profiles by a distance of 60 trailing edge momentum thicknesses. The location of y_m where the minimum velocity occurs is laterally displaced signifying that there is a net lateral (that is, downward) transfer of momentum within the wake. The calculations included in Fig. 4 show that the mean velocity profiles are overpredicted near the wake centerline and the predictions are reasonably good as the normal distance increases. Figure 5 shows the variation of spanwise component of mean velocity with

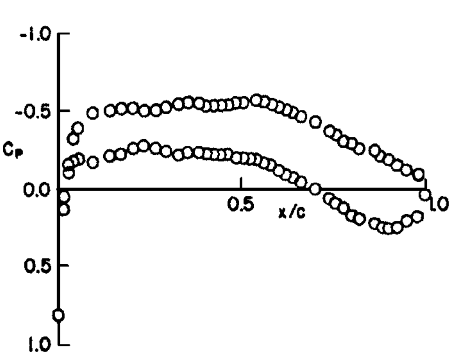

Fig. 3 Pressure distribution on the swept wing model.

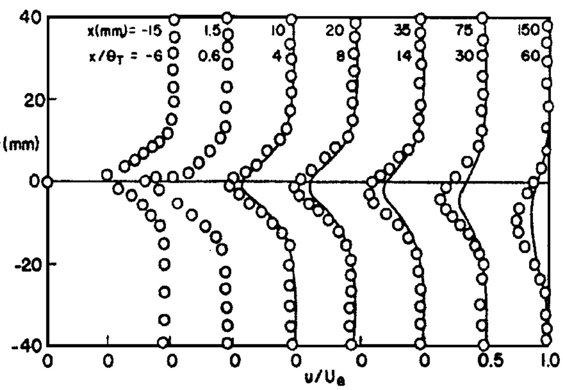

Fig. 4 Profiles of streamwise component of mean velocity: ○, experiment; and ——, computation.

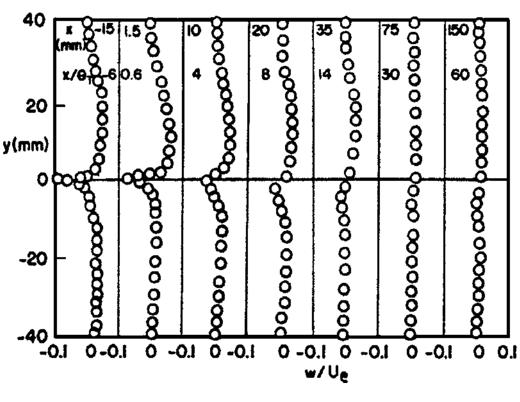

Fig. 5 Profiles of spanwise component of mean velocity.

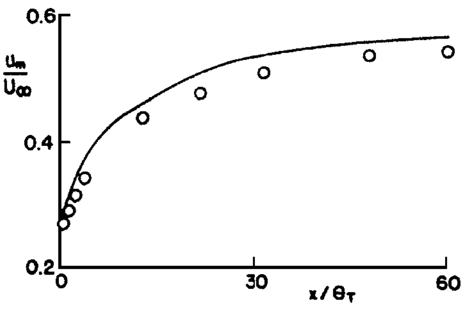

Fig. 6 Variation of minimum velocity in the near-wake: ○, experiment; and ——, computation.

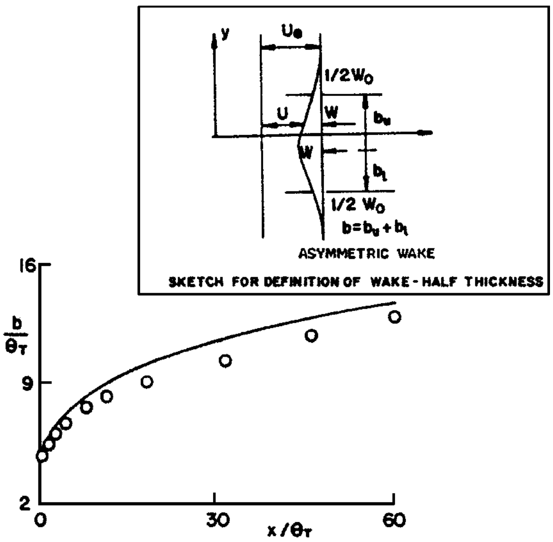

Fig. 7 Variation of wake half-thickness in the near-wake: ○, experiment; and ——, computation.

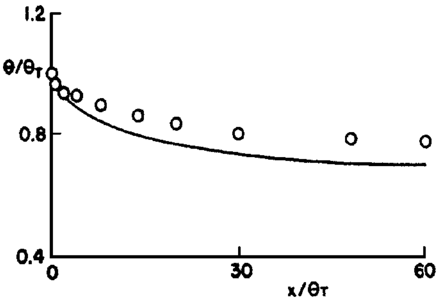

Fig. 8 Development of momentum thickness in the near-wake: ○, experiment; and ——, computation.

normal distance at various streamwise stations. It should be noted from the results of streamwise and spanwise components of mean velocity that the distance beyond which the profiles show a tendency for symmetrization is of the same order for both the velocity components.

Figures 6 and 7 show the development of minimum value of mean velocity and wake half-thickness with streamwise distance in the near-wake. Wake half-thickness b is the sum of the wake half-thicknesses on the upper and lower layers of the wake (see Fig. 7 for definition of b). Turbulent diffusion makes the wake half-thickness and minimum velocity increase rapidly with x/θ_T. Computed results presented in Figs. 6 and 7 show that the predictions are reasonably good near the trailing edge and as the streamwise distance increases the performance of the calculation scheme degenerates. Figures 8 and 9 show the development of momentum thickness and shape factor along the streamwise distance. The integration of the mean velocity profiles posed difficulties as a result of the asymmetry of the

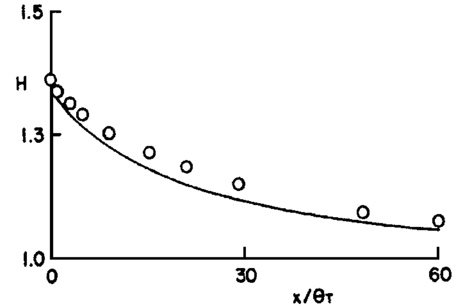

Fig. 9 Development of shape factor in the near-wake: ○, experiment and; ——, computation.

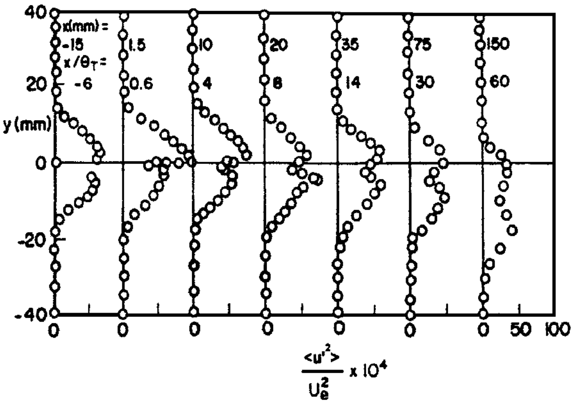

Fig. 10a Profiles of turbulent normal stress component $\langle u'^2 \rangle$.

wake profiles (that is, the external local mean velocity is not the same on either sides of the wake centerline). The value of the momentum thickness is obtained by integrating the mean velocity profile from minimum velocity position to maximum velocity position on either side of the minimum velocity line and adding the values obtained for both sides. One can observe a rapid decrease in the values of the momentum thickness near the trailing edge, and thereafter the momentum thickness is nearly constant. The shape factor (Fig. 9) evolves rapidly in the region upto $x/\theta_T = 30$, and thereafter the evolution is slow; by a distance of 60 trailing edge momentum thicknesses the shape factor is only slightly greater than 1, its asymptotic value at very large streamwise distances behind the trailing edge. Figures 8 and 9 show, also, that the predictions are good near the trailing edge, and as the distance from the trailing edge increases the predictions deteriorates. Figure 9 shows, also, that the initial rapid decrease in the distribution of shape factor has been captured by the calculation method suggesting that the neglect of the normal stress terms in the equations as well as the pressure gradients induced by the viscous-inviscid interactions can be justified.

The turbulent normal stresses $\langle u'^2 \rangle$, $\langle v'^2 \rangle$, $\langle w'^2 \rangle$ and the Reynolds shear stress components $\langle u'v' \rangle$ and $\langle u'w' \rangle$ in the near-wake are shown in Figs. 10–12. It is necessary to emphasize here that the Reynolds stress components are measured in the tunnel freestream direction, rather than in the streamline or other curvilinear coordinates. In a sense measurements made in this coordinate system are easier to use while computational results are compared with experimental data because most prediction methods for these flows would use a rectangular coordinate system. Figure 10a shows the streamwise turbulent normal stress distribution across the wake at different streamwise locations. It can be seen from the figure, for larger streamwise distances, that there are two maxima of $\langle u'^2 \rangle$ corresponding to the shear points on either sides of the minimum velocity line in the wake. Also it can be seen from the figure that the profiles close to the trailing edge (for smaller streamwise distances) are strongly asymmetric, and there is a tendency toward symmetrization by a distance of about 60 trailing edge momentum thicknesses. Figures 10b and 10c show the variation of turbulent normal stresses $\langle v'^2 \rangle$ and $\langle w'^2 \rangle$ across the wake at several streamwise locations. It

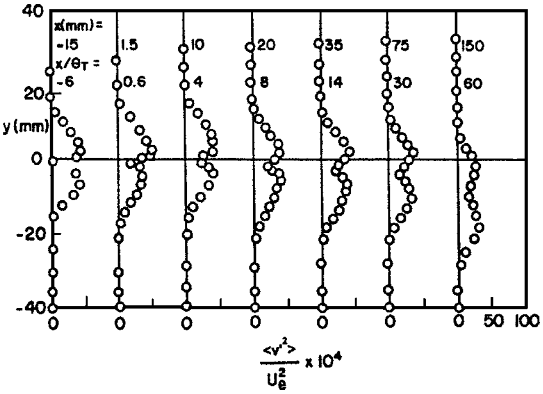

Fig. 10b Profiles of turbulent normal stress component $\langle v'^2 \rangle$.

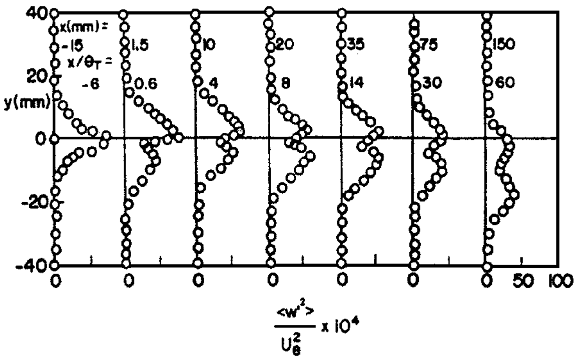

Fig. 10c Profiles of turbulent normal stress component $\langle w'^2 \rangle$.

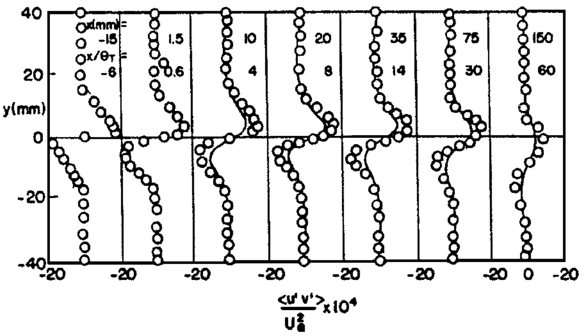

Fig. 11 Profiles of Reynolds-shear stress component $\langle u'v' \rangle$: ○, experiment; and ——, computation.

can be seen that the behavior of $\langle v'^2 \rangle$ and $\langle w'^2 \rangle$ in the wake is almost similar to that of $\langle u'^2 \rangle$ (Fig. 10a).

The development of Reynolds shear stress $\langle u'v' \rangle$ is shown in Fig. 11. The deviation from the antisymmetry in the profiles reduces as the streamwise distance increases. The zero crossing in the Reynolds stress profiles moves to the lower side and its location corresponds to the location of the minimum streamwise velocity component. Computed results presented in Fig. 11 show that the prediction of Reynolds-shear stress profiles is not good near the minimum velocity line. Figures 4 and 11 indicate a definite trend in the prediction of mean velocity and Reynolds-shear stress profiles. From the preceding results it can be concluded that there is a fair agreement between the predicted and measured results when the simplicity of the calculation procedure is kept in mind. Distributions of the Reynolds-shear stress component $\langle u'w' \rangle$ presented in Fig. 12 show that the development and decay of $\langle u'w' \rangle$ is almost similar to that of Reynolds stress component $\langle u'v' \rangle$. The maximum value of Reynolds stress component $\langle u'w' \rangle$ is about 20% of the maximum value of $\langle u'v' \rangle$. This result suggests that the streamlines are not strongly skewed, and there is only a weak correlation between the velocity components u and w, justifying the decision to make

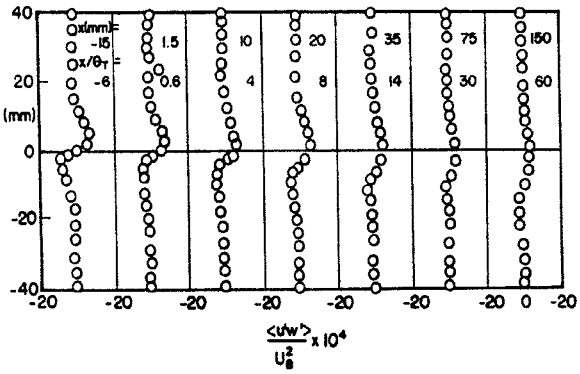

Fig. 12 Profiles of Reynolds-shear stress component $\langle u'w' \rangle$.

measurements along the tunnel freestream direction and not along the streamlines.

Results of minimum velocity, minimum value of $\langle u'^2 \rangle$ and $\langle u'v' \rangle$ zero crossing location show that the trajectories of these quantities move gradually toward the lower side of the wake, and these trajectories lie below the chord line. This is consistent with the trailing edge geometry of the airfoil used. It was observed from the results of minimum velocity, minimum value of streamwise turbulence intensity, and $\langle u'v' \rangle$ zero crossing location that the maximum difference among the trajectories of these quantities is less than 2 mm, and as the streamwise distance increases all three trajectories coincide.

The database, consisting of three mean velocity components, three turbulent normal stress components, and two Reynolds-shear stress components, generated in the present experimental study will be useful for testing the capabilities of various turbulence models, numerical prediction schemes, and validation of flow-solver codes, which take three-dimensionality of the flow into account.

Conclusions

A set of measurements, both mean and turbulence quantities, has been obtained in the three-dimensional turbulent near-wake behind an infinitely swept wing with a GAW(2) airfoil cross section in low speed flow. Profiles of mean velocity, turbulent normal stresses, and Reynolds shear stresses exhibit asymmetry close to the trailing edge and show a tendency toward symmetrization around a distance of 60 trailing edge momentum thicknesses. Engineering prediction of near-wake flow using the K–ε turbulence model has been carried out. The mean velocity and Reynolds-shear stress profiles are predicted reasonably well. Prediction of wake parameters is reasonably good close to the trailing edge, and the computations deteriorate as the streamwise distance increases. From this study it can be concluded that the agreement between the predictions and the experimental data is fair considering the simplicity of the engineering calculation scheme used for carrying out the computations. The near-wake flow studied here, being significantly three-dimensional and yet relatively simple, is expected to provide a broad understanding of asymmetric near-wake flow features and present a good and critical test of the capabilities of turbulence models, which take into account the three-dimensionality of the flow.

Acknowledgments

The authors gratefully acknowledge many useful discussions with P. R. Viswanath. Assistance rendered by the staff of the 1.5-m and boundary layer tunnels is acknowledged.

References

[1]Chevary, R., and Kovaznay, L. S. G., "Turbulence Measurements in the Wake of a Thin Flat Plate," *AIAA Journal*, Vol. 8, No. 9, 1969, pp. 1641–1647.

[2]Andreopolous, J., and Bradshaw, P., "Measurement of Interacting Turbulent Shear Layers in the Near-Wake of a Flat Plate," *Journal of Fluid Mechanics*, Vol. 100, 1980, pp. 639–652.

[3]Ramaprian, B. R., Patel, V. C., and Sastry, M. S., "Turbulent Wake Development Behind Streamlined Bodies," Univ. of Iowa, Iowa, U.S.A., IIHR Rept. 231, March 1981.

[4]Subaschandar, N., and Prabhu, A., "Development of Turbulent Near-Wake Behind an Infinitely Yawed Flat Plate," 95 FM 2, Dept. of Aerospace Engineering, Indian Inst. of Science, India, Feb. 1995.

[5]Novak, C. J., and Ramaprian, B. R., "Measurements in the Wake of an Infinite Swept Aerofoil," Univ. of Iowa, Iowa, U.S.A., IIHR Rep. No: 240, Sept. 1982.

[6]Subaschandar, N., and Prabhu, A., "Turbulent Near-Wake Development Behind a Flat Plate," *Journal of Aerospace Science and Technology*, Vol. 2, No. 2, 1999, pp. 61–81.

[7]Subaschandar, N., and Prabhu, A., "Analysis of Turbulent Near-Wake Development Behind an Infinitely Yawed Flat Plate," *International Journal of Non-Linear Mechanics*, Vol. 33, No. 6, 1998, pp. 1089–1102.

[8]Cousteix, J., and Pailhas, G., "Three-dimensional Turbulent wake behind swept wing," *Proceedings of Complex Turbulent Shear Flow*, edited by R. Dumas and L. Fulachier, Springer-Verlog, London, 1982, pp. 208–216.

[9]Sundaram, S., Viswanath, P. R., and Subaschandar, N., "Viscous Drag Reduction Using Riblets on a Swept Wing," *AIAA Journal*, Vol. 37, No. 7, 1999, pp. 851–856.

[10]Kline, S. J., and McClintock, F. A., "Describing Uncertainties in Single Sample Experiments," *Mechanical Engineering*, Vol. 75, No. 1, 1953, pp. 3–8.

[11]Subaschandar, N., and Prabhu, A., "An Engineering Prediction of Turbulent Near-Wake Behind an Infinitely Swept Wing," National Aerospace Lab., Rept. PD-EA-0014, Bangalore, India, Oct. 2000.